# Electromagnetic and Thermal Analysis of Interior Permanent Magnet Motors Using Filled Slots and Hairpin Windings

Dinh Bui Minh
School of Electrical Engineering
Hanoi University of Science and Technology
Hanoi, Vietnam
dinh.buiminh@hust.edu.vn

Hung Bui Duc
School of Electrical Engineering
Hanoi University of Science and Technology
Hanoi, Vietnam
hung.buiduc@hust.edu.vn

Nguyen Huy Phuong
School of Electrical Engineering
Hanoi University of Science and Technology
Hanoi, Vietnam
phuong.nguyenhuy@hust.edu.vn

Vuong Dang Quoc
School of Electrical Engineering
Hanoi University of Science and Technology
Hanoi, Vietnam
vuong.dangquoc@hust.edu.vn

**Abstract—This paper analyzes the electromagnetic and thermal design of interior permanent magnet motors using filled slots and hairpin windings for electric vehicle applications. Two models of ∇ shape of the interior permanent magnet motors have been proposed to evaluate the temperature distribution and cogging torque performance. A narrow opening slot of the interior permanent magnet of 48 slots/8 poles with the filled winding has been designed to investigate the electromagnetic torque because the cogging torque depends on opening stator slots. A parallel–rectangle slot of the interior permanent magnet with the hairpin winding has been also implemented with finite element analysis to evaluate their performances. Normally, the slot opening of the interior permanent magnet stator equals the slot width, it is greater than the size of hairpin windings, and the cogging torque is increased significantly with a bigger slot opening. The main advantage of the hairpin winding design is the high slot fill factors. Hence, the lower the current density, the higher torque, and efficiency are, than the normal design with the same geometry parameters. To improve the cogging torque due to the wide slot opening, the step–skew rotor slices have been arranged to minimize the torque ripple with different skewing angles.**

*Keywords-interior permanent magnet; finite element analysis; Ansys Maxwell; SPEED software; hairpin windings*

## I. INTRODUCTION

Hairpin-type windings are gaining increasing popularity [1, 2], especially in automotive traction motors due to advantages which include reduced manufacturing time, high fill factor, shorter end-winding overhang, and better high voltage protection. Moreover, with respect to the random nature and the packing style of traditional distributed windings, hairpin windings consist of a plurality of accurately placed stator bars [1, 3]. However, the cogging torque is very high with a wider slot opening, and it is also very complicated to manufacture.

Thus, in order to improve the torque ripple, a novel design of a step-skew V shape magnet has been presented for Interior Permanent Magnet (IPM) motors of 150kW (48 slots/8 poles). The stator stepped slot-openings with optimal shift angles have been implemented for the IPM motors in [4-6]. Cogging torque reduction has become an increasingly important issue in IPM motors. Effective methods for reducing the cogging torque, such as skewing slots, step-skewing rotor, and magnets are possible for the slot-filled windings. For the hairpin windings, only step-skewing rotor can be applied to improve the torque ripple. In this paper, a stepped skewing shift magnet rotor method for reducing the cogging torque of IPM motors, which can avoid the drawbacks of the wider slot opening of stator slots, is proposed. The electromagnetic torque and efficiency performance of the IPM motor are significantly affected by winding topology. The electromagnetic performance of multi-layered IPM motors keeping in mind their potential use in Electric Vehicle (EV) applications. The torque and back Electromagnetic Force (EMF) waveforms are verified with different step skewing models. The torque harmonics have been compared for different topologies. Finally, an IPM motor with a step-skewing magnet rotor is manufactured to verify the results of Finite Element Analysis (FEA) [9-12].

## II. HAIRPIN AND SLOT FILL WINDING DESIGNS

The designed IPM motor with ∇ shape of permanent magnet rotor with slot filled and hairpin windings is presented in Figure 1. The stator slot parameters are pre-determined in and are shown in Table I. The slot-filled winding has an opening width of 1.2mm, which is greater than the wire diameter of 1mm (Figure1(a)) and the stator slot opening of the hairpin winding is 5mm, bigger than the rectangle bar sizes of 4.3×3.3mm (Figure 1(b)).
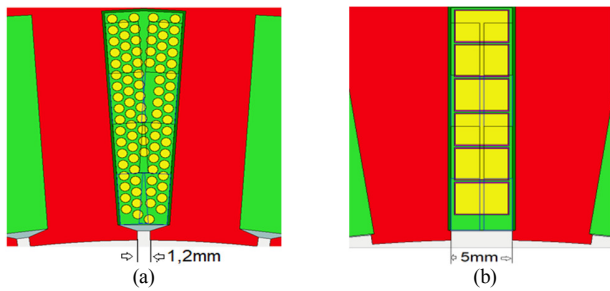
Fig. 1.     (a) Slot filled winding and (b) hairpin winding.

TABLE I.     SLOT FILLED AND HAIRPIN WINDING PARAMETERS

| Parameter | Unit | Slot filled winding | Harpin winding |
|---|---|---|---|
| Stator lamination diameter | mm | 250 | 250 |
| Stator bore $D_s$ | mm | 175 | 175 |
| Airgap | mm | 1 | 1 |
| Stator slot opening width ($t_S$) | mm | 1.2 | 5 |
| Mechanical opening angle | (0) | 0.55 | 2.22 |
| Motor length | mm | 240 | 240 |
| Stator lam length | mm | 120 | 120 |
| Magnet length | mm | 120 | 120 |
| Magnet Segments | | 6 | 6 |
| Rotor lam length | mm | 100 | 100 |
| EWG Overhang [F] | mm | 55 | 37 |
| EWG Overhang [R] | mm | 55 | 37 |
| Copper size | mm | Φ 0.85 | 4.3×3.3 |
| Number strands | | 15 | 1 |
| Phases | | 3 | 3 |
| Turns | | 6 | 6 |
| Throw | | 5 | 5 |
| Parallel paths: | | 2 | 2 |

The two IPM motors have 48 slot/8poles, the stack length is 51mm, the diameter of stator and rotor is 250mm and 175mm respectively, the air-gap length is 1mm, the thickness of the electrical steel sheet is 0.2mm, the continuous phase current amplitude is 400A, the continuous rated power is 150kW, and the maximum speed of the machines is 12000rpm. The main differences are winding overhang, slot opening, and the copper sizes of 15 (Φ 0.85) and 4.3×3.3mm. The slot opening is 1.2mm in slot filled and 5mm in hairpin designs. In both models, the slot openings are arranged along the motor axis and the central position of the slots remains the same. The cogging torque of IPM motors results from the interaction between the stator teeth and rotor magnetic poles, which can be expressed in Fourier series [6-8]:

$$T_{cg} = \sum_{i=0}^{n} T_{c,i} \sin(iN\theta) \quad (1)$$

where $i$ is the order of the cogging torque harmonics, $T_{ci}$ is the amplitude of $i$ order cogging torque component, and $N$ is the least common multiple between the number stator slots and rotor poles. The mechanical angle of the stator opening $\theta$ is:

$$\theta = 360 \frac{t_S}{\pi D_S} \quad (2)$$

where $t_S$ is slot opening width, $D_S$ is the stator diameter.

The cogging torque of slot filled winding with 1.2mm ($0.55^0$) opening is 2.8N.m, while the cogging torque of Hairpin winding with 5mm opening width ($2.22^0$) is 8N.m, which is three times bigger than the slot filled winding designs.
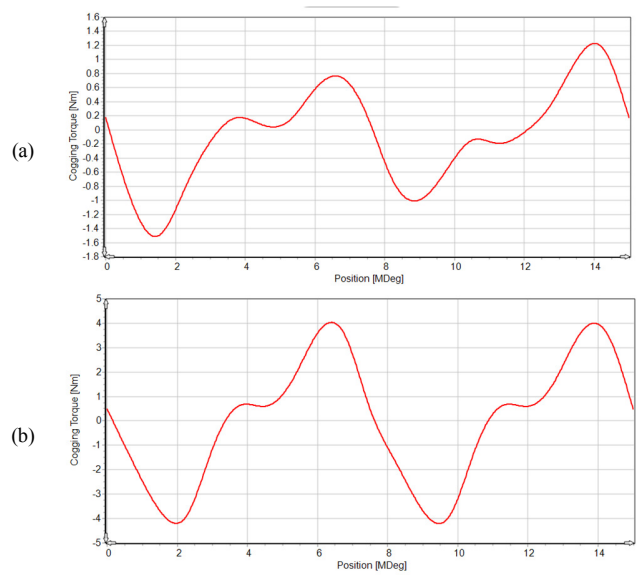


Fig. 2.     (a) Cogging torque of slot filled and (b) hairpin winding.

III.     COGGING TORQUE AND THERMAL ANALYSIS

To eliminate the cogging torque by the stator slot-openings, the step-skewing rotor has a shift angle of $\beta$ mechanical degrees. The cogging torque can be transformed as [6]:

$$T_{cog} = \sum_{i=0}^{n} T_{ci} \sin(iN(\theta - \beta)) \quad (3)$$

If the rotor is divided into segments along the motor axial direction, and the relative shift angle between the adjacent two rotor poles is $\delta_n$ mechanical degrees, the resultant cogging torque can be expressed as [6]:

$$T_{cog} = \sum_{i=1}^{n} T_{ci} \sum_{j=0}^{n-1} . \sin(iN(\theta - j\beta_n)) \quad (4)$$

The above equation can be simplified to:

$$T_{cog} = \frac{1}{n} \sum_{i=1}^{n} T_{ci} \frac{\sin \frac{iN\beta_n n}{2}}{\sin \frac{iN\beta_n}{2}} \sin(iN(\theta - j\beta_n)) \quad (5)$$

Hence, for eliminating the $i$-th order cogging torque component, the theoretical shift angle $\beta_n$ must fulfill the following requirements:

$$\sin \frac{iN\beta_n n}{2} = 0 \quad (6)$$

By applying the cogging torque for straight skewing and V-shape skewing magnet model, the conventional skewing model with straight skewing has a smaller shift angle than the V-shape skewing model with the same total skewing angle. The V shape magnet model has more advantages than the straight skewing because two harmonic orders can be eliminated together. For example, the harmonic orders with mechanical degrees of $1^0$ or $3^0$ are reduced to zero if they fulfill (6). The cogging torque of the 3 models is shown in Figure 3. The cogging torque of the V shape skewing design is the lowest value because the second order harmonics are eliminated in this model. The back EMF harmonic of the 3 models has been analyzed by Fourier transform from the electromagnetic force waveform with the harmonic order from the first to the 15th order. The back EMF amplitude versus harmonic order was implemented by the

Matlab function to obtain the results shown in Figure 5. From the back EMF harmonic result, the total harmonic distortion TDH of Model 3 with V skewing is the smallest about 4.2%.
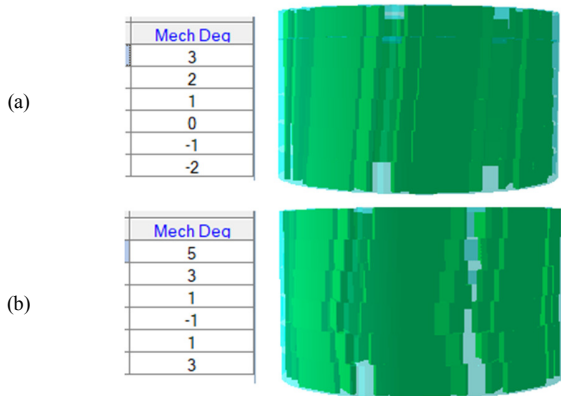


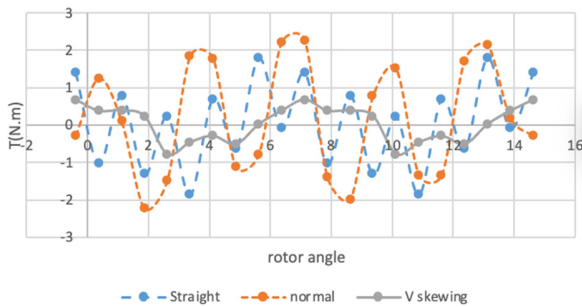Fig. 3.     (a) Straight skewing and (b) V-skewing.
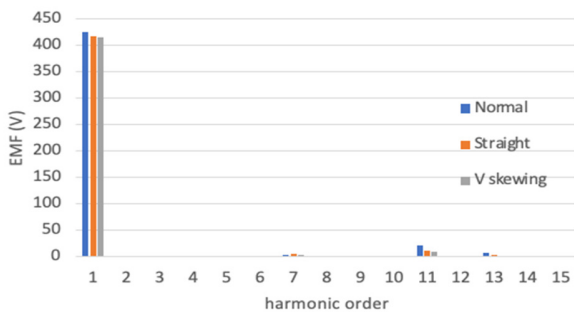


Fig. 4.     Cogging torque of the 3 models.



Fig. 5.     Back EMF harmonic order analysis of the models.

The temperature distribution of slot fill and hairpin winding designs is depicted in Figure 6. The hot spot of Hairpin winding is $105.7^0$C, which is lower than $111.5^0$C. Based on these results, the IPM V skewing with the hairpin winding design is preferable for EV applications. The efficiency map of hairpin winding design is shown in Figure 7, with a speed range of 12000rpm and a current density of $8.9$A/m$^2$.

## IV.     SKEWING ROTOR DESING

The prototype with the 6-segmented magnets has been manufactured and is shown in Figure 8. Each segment with a thickness of 20mm is skewed by 1.5 mechanical degrees. To insert the six segments simply, every segment block is

designed with one guide pin to fix the correct position when all segments assembly together.
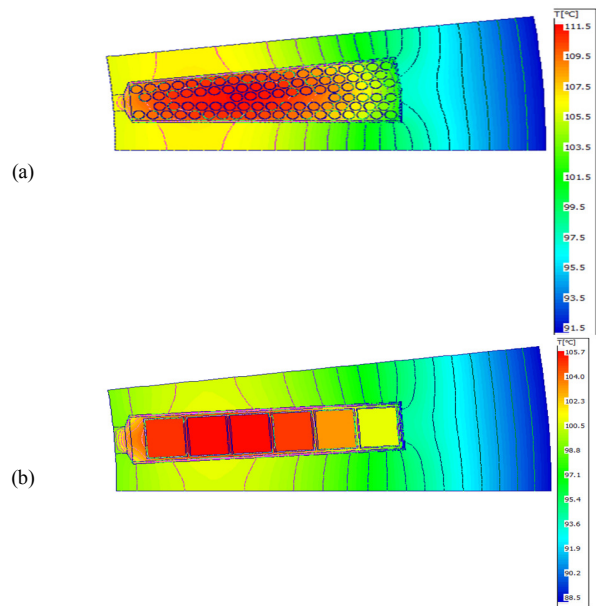


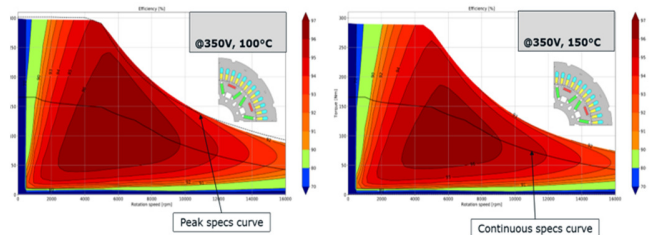Fig. 6.     (a) Slot fill, (b) hairpin winding designs temperature distribution.



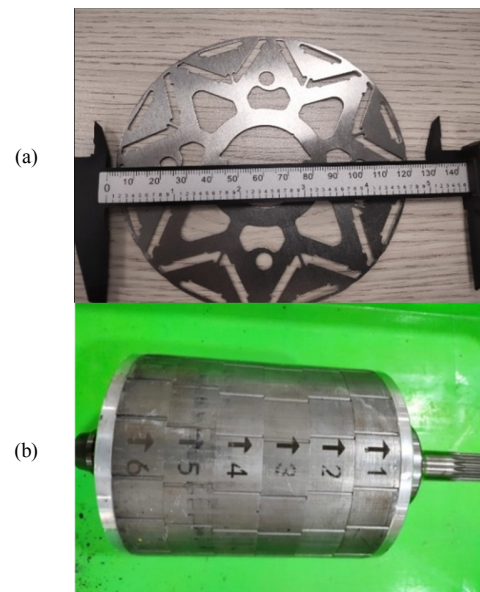Fig. 7.     Efficiency map of hairpin winding design.



Fig. 8.     (a) Rotor lamination, (b) Six step-V skew magnet slices assembly.

The whole hardware of the IPM motor has been assembled as in Figure 9. The high accurate torque transducer is used to measure the torque and speed values under different load conditions. The measured no-load phase EMF at 1500rpm of IPM is shown in Figure 10. To verify the electromagnetic performance, the 48 slot/8 pole proposed PM machine is built. Distributed windings were adopted. It should be noted that the PM motor is a prototype. The no-load back-EMF is carried out by using a voltage sensor. The simulated and measured results are exhibited in Figure 10. One circle of the back EMF has been measured by the oscilloscope and the data were recorded for plotting those curves.
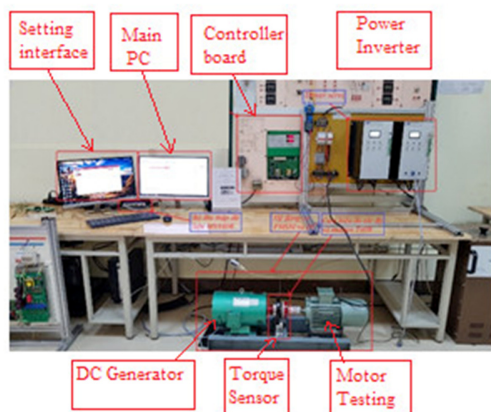


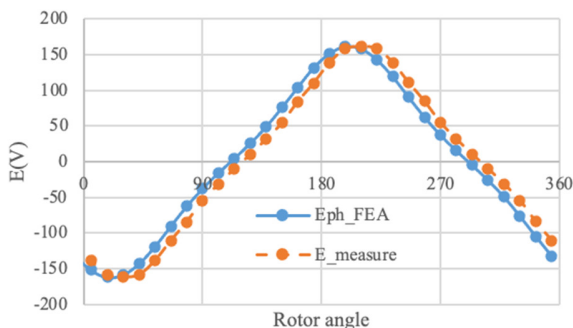Fig. 9.     Back EMF measurement of the IPM motor system.



Fig. 10.     Back EMF comparison of IPM motor system.

## V.     CONCLUSION

The obtained performance of IPM with slot filled and hairpin windings in the wide speed range has been presented in this paper and the effect of slot opening width on the cogging torque has been discussed. The thermal simulation of the two designs has been investigated to find out the hot spot or maximum temperature of hairpin and slot filled windings. A significant contribution of this study is the analytical calculation of the V skewing angle for the elimination of the second order harmonics of the cogging torque. A prototype of the V skewing magnet shape of the IPM hairpin winding has been manufactured and assembled. The simulation results achieved peak torque of 300N. m at the base speed of 5500rpm. The back EMF waveforms obtained from the FEA are close to the measured ones.

REFERENCES

[1]  C. Liu *et al.*, "Experimental Investigation on Oil Spray Cooling With Hairpin Windings," *IEEE Transactions on Industrial Electronics*, vol. 67, no. 9, pp. 7343–7353, Sep. 2020, https://doi.org/10.1109/TIE. 2019.2942563.

[2]  J.-W. Chin, K.-S. Cha, M.-R. Park, S.-H. Park, E.-C. Lee, and M.-S. Lim, "High Efficiency PMSM With High Slot Fill Factor Coil for Heavy-Duty EV Traction Considering AC Resistance," *IEEE Transactions on Energy Conversion*, vol. 36, no. 2, pp. 883–894, Jun. 2021, https://doi.org/10.1109/TEC.2020.3035165.

[3]  J.-G. Lee, H.-K. Yeo, H.-K. Jung, T.-K. Kim, and J.-S. Ro, "Electromagnetic and thermal analysis and design of a novel-structured surface-mounted permanent magnet motor with high-power-density," *IET Electric Power Applications*, vol. 13, no. 4, pp. 472–478, Jan. 2019, https://doi.org/10.1049/iet-epa.2018.5322.

[4]  J. Zhao, J. Wang, L. Zhou, W. Huang, Y. Ma, and Z. Zhang, "Cogging Torque Reduction by Stepped Slot-Opening Shift for Interior Permanent Magnet Motors," in *2019 22nd International Conference on Electrical Machines and Systems (ICEMS)*, Harbin, China, Dec. 2019, https://doi.org/10.1109/ICEMS.2019.8921448.

[5]  S.-K. Lee, G.-H. Kang, J. Hur, and B.-W. Kim, "Stator and Rotor Shape Designs of Interior Permanent Magnet Type Brushless DC Motor for Reducing Torque Fluctuation," *IEEE Transactions on Magnetics*, vol. 48, no. 11, pp. 4662–4665, Aug. 2012, https://doi.org/10.1109/ TMAG.2012.2201455.

[6]  X. Ge, Z. Q. Zhu, G. Kemp, D. Moule, and C. Williams, "Optimal Step-Skew Methods for Cogging Torque Reduction Accounting for Three-Dimensional Effect of Interior Permanent Magnet Machines," *IEEE Transactions on Energy Conversion*, vol. 32, no. 1, pp. 222–232, Mar. 2017, https://doi.org/10.1109/TEC.2016.2620476.

[7]  G. Pellegrino, A. Vagati, and P. Guglielmi, "Design Tradeoffs Between Constant Power Speed Range, Uncontrolled Generator Operation, and Rated Current of IPM Motor Drives," *IEEE Transactions on Industry Applications*, vol. 47, no. 5, pp. 1995–2003, Sep. 2011, https://doi.org/ 10.1109/TIA.2011.2161429.

[8]  G. Pellegrino, A. Vagati, P. Guglielmi, and B. Boazzo, "Performance Comparison Between Surface-Mounted and Interior PM Motor Drives for Electric Vehicle Application," *IEEE Transactions on Industrial Electronics*, vol. 59, no. 2, pp. 803–811, Oct. 2012, https://doi.org/ 10.1109/TIE.2011.2151825.

[9]  M. Barcaro, N. Bianchi, and F. Magnussen, "Design considerations to maximize performance of an IPM motor for a wide flux-weakening region," in *The XIX International Conference on Electrical Machines - ICEM 2010*, Rome, Italy, Sep. 2010, https://doi.org/10.1109/ ICELMACH.2010.5607926.

[10] V. D. Quoc, "Robust Correction Procedure for Accurate Thin Shell Models via a Perturbation Technique," *Engineering, Technology & Applied Science Research*, vol. 10, no. 3, pp. 5832–5836, Jun. 2020, https://doi.org/10.48084/etasr.3615.

[11] D. B. Minh, L. D. Hai, T. L. Anh, and V. D. Quoc, "Electromagnetic Torque Analysis of SRM 12/8 by Rotor/Stator Pole Angle," *Engineering, Technology & Applied Science Research*, vol. 11, no. 3, pp. 7187–7190, Jun. 2021, https://doi.org/10.48084/etasr.4168.

[12] D. B. Minh, V. D. Quoc, and P. N. Huy, "Efficiency Improvement of Permanent Magnet BLDC Motors for Electric Vehicles," *Engineering, Technology & Applied Science Research*, vol. 11, no. 5, pp. 7615–7618, Oct. 2021, https://doi.org/10.48084/etasr.4367.